12

Intraplate seismic hazard: Evidence for distributed strain and implications for seismic hazard

SUSAN E. HOUGH

Abstract

In contrast to active plate boundaries, the lack of a fundamental scientific framework to understand seismogenesis combines with the lower rates of earthquakes to make probabilistic seismic hazard assessment (PSHA) challenging in intraplate regions. Seismic hazard maps for intraplate regions tend to indicate hazard dominated by source zones that have produced large earthquakes during historical times. The level of hazard can also depend critically on the magnitudes of pre-instrumental earthquakes, which are clearly far less certain than earthquakes during the instrumental era. In this brief chapter I first summarize recently published results that address the long-standing paradox of low strain accrual and high moment release in the Central/Eastern United States (CEUS); I then summarize recent published studies from the CEUS and elsewhere suggesting that strain release is more spatially distributed over timescales of millennia to tens of millennia than over the past few centuries. I explore a simple quantitative model that has been discussed in numerous past studies, namely that strain is everywhere low, with weak modulation in the CEUS due to glacial isostatic adjustment and concentration within failed rifts that represent large-scale zones of weakness in the crust. Within this paradigm, one can consider an overall moment-release budget associated with low but spatially distributed strain. I show that even a conservative estimate of strain rate ($0.5–1.0 \times 10^{-9}$/yr) can generate the rate of moment release observed in historical times, if the strain is distributed and large historical earthquakes were close to M_w 7.0. Basic considerations from both geological observations and statistical seismology support the assumption that, over decadal to century timescales, activity is likely to remain concentrated in areas that have seen elevated activity in the recent geological past. Significant rate changes are possible, however, over short timescales, and may be likely over millennial scales –

Intraplate Earthquakes, ed. Pradeep Talwani. Published by Cambridge University Press.

as demonstrated, in addition to other evidence discussed in this paper, by abundant and widely accepted evidence that the New Madrid seismic zone itself "turned on" in the relatively recent geological past. One logic-tree approach to PSHA might therefore be to include a low probability that recent clusters have ended along with a non-zero probability that future activity within other rifted zones will exceed the rate predicted by an extrapolation of current background rates.

12.1 Introduction

Quantifying probabilistic seismic hazard remains a vexing problem in intraplate regions throughout the world. Along active plate boundary regions, expected long-term earthquake rates can be estimated from seismicity catalogs, geological evidence of past earthquakes, and GPS estimates of ongoing deformation. Hazard assessment remains challenging, and under active investigation, even in active regions (e.g., WGCEP, 2013); however, in a well-studied region such as Japan or California, geological results and deformation data provide at least a first-order constraint on seismic moment accrual and release rates. The magnitude of the maximum possible earthquake in a region, M_{max}, can also be estimated given an overall strain rate, paleoseismic constraints on the rate of surface-rupturing earthquakes, and the commonly accepted assumption that, in most regions if not for specific faults, regional earthquake magnitudes follow a Gutenberg–Richter distribution (Gutenberg and Richter, 1944; King, 1983; Felzer, 2006; Hough, 1996).

In intraplate regions, estimation of long-term earthquake rates is far more challenging. A fundamental difficulty for hazard assessment is that, unlike active plate boundary zones, no basic, integrated physical framework can explain the first-order processes controlling seismogenesis in intraplate regions. Given the lower rate of earthquakes, even relatively long historical catalogs are inadequate to capture long-term average rates; direct geological evidence of past earthquakes is generally scant, and hopes of constraining low strain rates from GPS data have not generally been borne out to date, with improved data often revealing little to no detectable surface deformation (e.g., Calais *et al*., 2005; Frankel *et al*., 2012). With no long-term constraint on fault slip rate or deformation from geological or geodetic data, estimates of earthquake rates and thus hazard are estimated from seismicity data; i.e., the earthquakes observed during historic times and/or documented in prehistoric times, and their estimated magnitudes. Even where the largest known earthquakes – the M_{max}, or characteristic earthquakes – occurred during pre-instrumental times, magnitude estimates can be uncertain by a full magnitude unit or more (see Hough and Page, 2011). Recurrence times for an assumed characteristic event can sometimes be estimated from geological evidence; however, as I discuss in a later section, even these long-term recurrence rate estimates are highly uncertain in intraplate regions.

In this chapter I focus initially on our current understanding of seismic hazards in the Central/Eastern United States (CEUS), where (1) large earthquakes have struck in historical

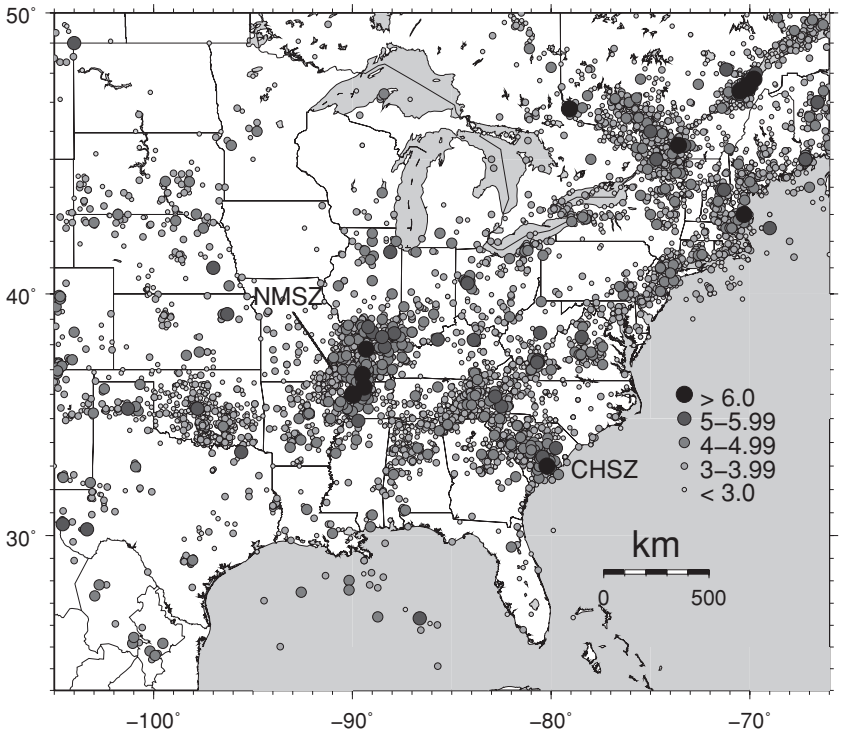

Figure 12.1 CEUS earthquake catalog determined for the CEUS SSC Project (Coppersmith *et al*., 2012). The CEUS-SSC Catalog is modified to include a M5.2 inferred triggered earthquake near Louisville, Kentucky, which occurred at 10:40 LT on February 7, 1812 (Hough, 2001), and to revise the magnitude of the 1843 Marked Tree, Arkansas, earthquake from 6.0 to 5.4 (Hough, 2013).

times, (2) GPS results provide an increasingly tight (and low) bound on strain accrual rates, and (3) extensive research has focused on both the magnitudes and the recurrence rates of the (assumed) characteristic earthquakes. Moreover, efforts to understand intraplate seismogenesis, both in the CEUS and more generally, have focused largely on reconciling the apparent paradox posed by high rates of moment release versus a low rate of strain accrual. Research results to date as well as the conclusions of this chapter are expected to have general applicability for low strain rate regions, although, as I discuss later in the chapter, there appear to be some differences in the nature of seismicity characteristics between intraplate regions.

12.2 Seismic moment release in the Central/Eastern United States

12.2.1 Historical earthquakes: introduction and rupture scenarios

Moderate earthquakes have occurred in many regions in the CEUS during the ~300-year historical record (Figure 12.1). However, according to all recent characterizations, overall

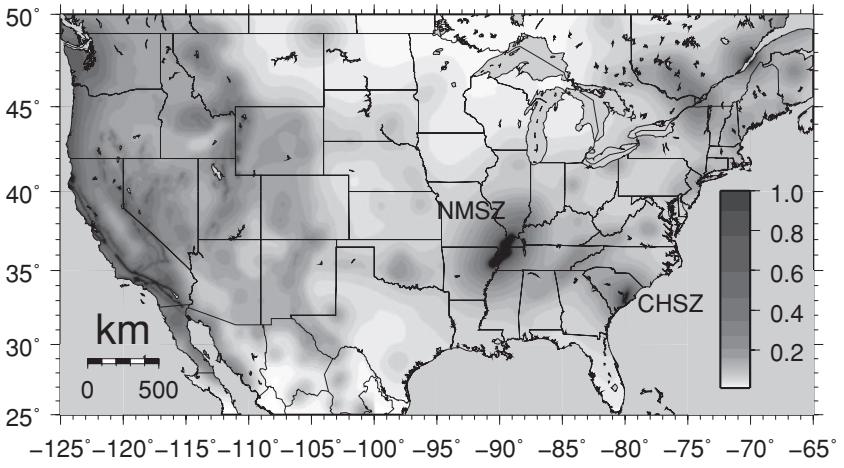

Figure 12.2 National Seismic Hazard Mapping Program seismic hazard map for the United States: PGA (%g) with 2% probability of exceedence in 50 years, rock site (grayscale) (results from Petersen *et al*., 2008).

moment release in the region has been concentrated in two source zones: the New Madrid, Central United States, seismic zone (NMSZ) and the Charleston, South Carolina, seismic zone (CHSZ) (Figure 12.2). Because of low regional attenuation (e.g., Nuttli, 1973a), the NMSZ) contributes significantly to seismic hazard in relatively distant, large midwestern United States cities such as St. Louis, Missouri (Frankel *et al*., 2002; Petersen *et al*., 2008). I note that, in general, low attenuation will be a key factor contributing to seismic hazard estimates in intraplate regions; the focus of this chapter, however, is on issues related to source characterization. The CHSZ also contributes significantly to regional as well as local hazard estimates. Away from the NMSZ and CHSZ, the likelihood of a large ($M \geq 7$) earthquake is low, typically estimated by extrapolating background seismicity rates assuming a Gutenberg–Richter distribution with an imposed M_{max}.

Given the importance of the NMSZ and CHSZ for probabilistic seismic hazard analysis (PSHA) in the CEUS, considerable effort has been devoted to understanding the large earthquakes that occurred in both regions during historical times. Decades of painstaking investigations have led to the development of detailed rupture scenarios for both the 1811–1812 New Madrid earthquake sequence and the 1886 Charleston earthquake. For the NMSZ, available data include (1) paleoliquefaction features preserved by the sediments within the Mississippi Embayment (e.g., Tuttle and Schweig, 1996); (2) the present-day distribution of seismicity in the NMSZ, which has commonly been assumed to be a long-lived aftershock sequence that illuminates the principal fault zones (e.g., Gomberg, 1993; Johnston, 1996; Mueller *et al*., 2004; Ebel *et al*., 2000; Stein and Liu, 2009); (3) first-hand reports ("felt reports") of the shaking and/or damage caused by the events over the CEUS (e.g., Nuttli, 1973b; Street, 1982, 1984).

The 1811–1812 New Madrid earthquake sequence comprised four principal earthquakes that occured over 3 months. By some accounts the principal events in this sequence are

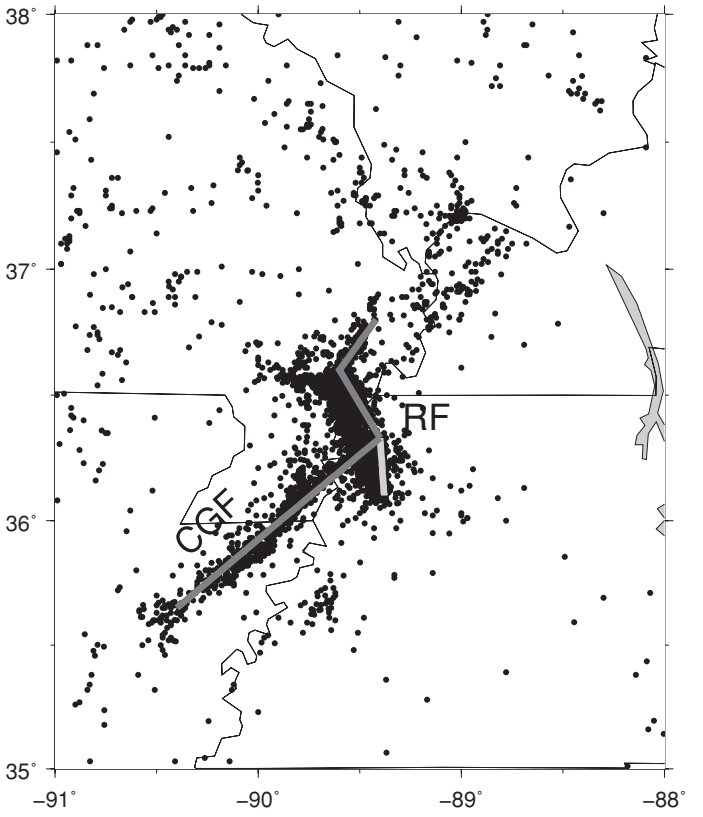

Figure 12.3 New Madrid seismic zone, including instrumentally recorded seismicity (black dots) and inferred traces of the Cottonwood Grove fault (gray line; CGF) and Reelfoot fault (gray line; RF). The location of the northern limb of the NMSZ is also indicated (gray line extending northeastward from the northern end of the RF).

among the largest – if not the largest – earthquakes to have ever occurred in a so-called Stable Continental Region (SCR; Johnston, 1996). Ground motions from the principal events were felt by individuals as far away as Canada, New England, and at a number of locations along the Atlantic coast (Mitchill, 1815; Fuller, 1912; Nuttli, 1973b; Street, 1982, 1984; Johnston, 1996). Contemporary accounts document three principal mainshocks: approximately 2:15 a.m. local time (LT) on December 16, 1811; around 8:00 a.m. LT on January 23, 1812, and approximately 3:45 a.m. LT on February 7, 1812 (henceforth NM1, NM2, and NM3, respectively). Additionally, a large aftershock to NM1 (NM1-A) occurred near dawn on December 16, 1811. There is some documentation of energetic aftershock sequences following each mainshock (Drake, 1815; McMurtie, 1819; Hough, 2009).

As noted, rupture scenarios have been developed for the four principal 1811–1812 events based on a number of lines of evidence (e.g., Johnston and Schweig, 1996; Figure 12.3). Of these, the association of NM3 with the Reelfoot thrust fault is the best supported by direct

evidence, including the appearance of waterfalls along the Mississippi River (e.g., Russ, 1982; Odum *et al*., 1998). NM1 is commonly associated with the strike-slip Cottonwood Grove fault, largely based on the prominent lineation illuminated by microseismicity as well as the distribution of liquefaction. Direct evidence from written archival accounts points only to a location somewhere south of the Reelfoot fault; i.e., unlike NM3, there are no accounts suggestive of surface rupture or accounts suggesting near-fault effects (e.g., localized extremely strong ground motions). The rupture scenario for NM1A is similarly uncertain. Two different scenarios have been proposed for NM1A: a rupture on the northern Cottonwood Grove strike-slip fault (Johnston and Schweig, 1996), or a rupture on the southeastern extension of the Reelfoot thrust fault (Hough and Martin, 2002). For this event direct evidence – the shaking distribution as inferred from written accounts – suggests only a location to the north of NM1. The rupture scenario of NM2 is the least well constrained: although associated by most authors with strike-slip motion on the northern limb of the NMSZ (e.g., Johnston and Schweig, 1996), Mueller *et al*. (2004) and Hough *et al*. (2005) summarize several lines of evidence from written accounts suggesting the event might have been centered in the Wabash Valley, well north of the NMSZ, in a region where a contemporaneous account describes "wagon loads" of sand erupting at the surface during the 1811–1812 sequence (although the account does specify when in the sequence the sand blows occurred).

Owing to the incomplete historical and paleoseismic records, the various 1811–1812 rupture scenarios and our general understanding of the NMSZ are heavily guided by the distribution and interpretation of present-day seismicity; I therefore now review this issue briefly. The long-lived aftershock hypothesis (e.g., Ebel *et al*., 2000; Stein and Liu, 2009) has recently been called into question by Page *et al*. (2012), who used simulated sequences based on the epistemic triggering of aftershock (ETAS) model to show that no plausible set of sequence parameters can explain the robust known features of the early 1811–1812 aftershock sequence and the current rate of small earthquakes, assuming them to be aftershocks. It remains unclear, then, why present-day background seismicity does appear to illuminate the primary 1811–1812 ruptures. One might question this assumption; however, there is no question that present-day microseismicity illuminates the Reelfoot fault and, as noted, there is compelling evidence that this fault produced NM3. It reasonably follows, then, that microseismicity may well illuminate the overall sequence. An alternative hypothesis is that present-day microseismicity is driven by low levels of deep creep on continuations of faults below the brittle seismogenic crust, as Frankel *et al*. (2012) conclude is occurring on the Reelfoot and that perhaps continues at lower levels on the Cottonwood Grove fault. This would explain why the seismicity pattern of the NMSZ, with its well-defined side limbs, is consistent with predicted Coulomb stress increase associated with mainshock rupture on these two faults (Mueller *et al*., 2004). (So far as we know, the temporal decay of aftershocks universally follows Omori's law (e.g., Omori, 1895). Since rigorous statistical tests reveal that NMSZ seismic activity since the early nineteenth century cannot be explained by Omori's law (Page *et al*., 2012) and are therefore not aftershocks, a plausible alternative hypothesis is that ongoing creep at depth is not a consequence of post-seismic

deformation, but rather is a steady-state process that drives both background seismicity as well as occasional large earthquakes.) In either case, any inference of rupture length for a historical earthquake based on present-day microseismicity patterns is clearly uncertain. A defensible alternative constraint on rupture length, for example, discussed in detail by Mueller *et al*. (2004) and Hough and Page (2011), is that NM3 rupture was bounded by the intersection with the northern and southern limbs of the NMSZ (Figure 12.3) rather than the significantly longer rupture length assumed by a number of other researchers (e.g., Johnston and Schweig, 1996; Frankel *et al*., 2012). I discuss this issue at more length in a later section.

The Charleston earthquake of September 1, 1886 – 9:50 p.m. LT on August 31, 1886 – was the primary event in an apparently more typical earthquake sequence: a single large mainshock preceded by a small number of foreshocks and followed by a conventional, although spatially distributed, aftershock sequence (Dutton, 1889; Seeber and Armbruster, 1987). As discussed by Hough (2004), the overall felt extent of the mainshock was similar to that of the principal 1811–1812 New Madrid earthquakes, although far better sampled by extant archival accounts. As summarized by Talwani and Dura-Gomez (2009) and Dura-Gomez and Talwani (2009), available geophysical data combined with precise locations of present-day seismicity reveals a complex fault system including the northeast-striking Woodstock fault, an oblique right-lateral strike-slip fault with a ~6 km long antidilational left step through which the Sawmill Branch fault is the most active. As discussed by Dura-Gomez and Talwani (2009), detailed contemporary accounts point to the involvement of multiple faults, likely including the Woodstock fault, in the 1886 Charleston mainshock. Proposed rupture scenarios for this earthquake have been less detailed than those discussed above for the 1811–1812 New Madrid sequence. Recent microseismicity does not appear to delineate the historical mainshock rupture, and extensive liquefaction, as documented initially by Dutton (1889) and later by Talwani and Schaeffer (2001) is distributed over a broad source zone.

12.2.2 Historical earthquakes: magnitudes

The magnitudes of the principal 1811–1812 earthquakes are of critical importance for hazard assessment and efforts to understand intraplate seismogenesis. As discussed by numerous past studies (see Johnston and Schweig, 1996, for summary), inferred rupture scenarios and the size and distribution of liquefaction features provide some constraint on magnitude. There is no question that both the 1811–1812 mainshocks and the 1886 Charleston earthquake generated extensive liquefaction (e.g., Fuller, 1912; Obermeier *et al*., 1990; Saucier *et al*., 1991; Tuttle *et al*., 2002; Dutton, 1889; Talwani and Cox, 1985). Widespread and enormous sand blows such as those in the NMSZ provide prima facie evidence for large magnitudes. However, such magnitude estimates are not well constrained (e.g., Pond and Martin, 1997; Stein and Newman, 2004). Recently, Holzer *et al*. (2011) presented preliminary results from a new method to estimate peak ground acceleration (PGA) from cone penetration test soundings, concluding that PGA values in the liquefaction zone of

the 1811–1812 sequence were in the range 0.2–0.46 g. Holzer *et al*. (2011) state that these moderate-to-high values are consistent with $M_w \approx 7.5$ values and inconsistent with magnitudes smaller than 7. However, predicted accelerations at deep-sediment sites for earthquakes of M_w 7.0 and larger are uncertain in intraplate regions owing to a lack of direct observation. For example, the preliminary results of Ramirez-Guzman *et al*. (2011a), based on ground motion simulations, reveal perhaps surprising insensitivity of predicted intensities within the embayment, at distances over which significant liquefaction occurred, to magnitude values ranging from 7.0 to 7.7. That is, over this range of magnitudes, predicted intensities do not vary enough to be useful as a discriminant given the uncertainties in observed intensity values. Noting this uncertainty, Ramirez-Guzman *et al*. (2011b) suggest that predicted shaking intensities within the Mississippi Embayment will not be useful to constrain historical earthquake magnitudes within the range 7.0 to 7.7, and conclude that additional constraints, "such as those provided by paleoliquefaction analyses," will be needed to reduce uncertainties in magnitude estimates. However, while the distribution and size of liquefaction features might conceivably shed further light on magnitudes, the method developed by Holzer *et al*. (2011) uses paleoliquefaction analysis to derive ground motions, the interpretation of which will be plagued by the same uncertainties documented by Ramirez-Guzman *et al*. (2011a, b).

In light of these uncertainties, determination of magnitudes for the 1811–1812 mainshocks has thus hinged critically on the felt reports and the interpretation of associated modified Mercalli intensity (MMI) values by various investigations. Magnitude estimates have varied enormously, from ~7 (Hough and Page, 2011) to as high as 8¾ (Nuttli, 1979). Values close to M_w 7 have also been suggested based on constraints on the overall present-day strain rate (e.g., Newman *et al*., 1999), although inference of magnitude from strain rate is highly model-dependent (e.g., Kenner and Segall, 2000). While different analyses of macroseismic data from the New Madrid sequence have yielded widely varying magnitude estimates, underscoring the inherent difficulty in assessing historical earthquake records, in all studies the four principal events are found to have roughly comparable magnitudes, with a range of at most 1 magnitude unit. For the maps released by the U.S. Geological Survey National Seismic Hazard Mapping Project (NSHMP) in 2002, values of 7.3–8.0 were considered using a logic-tree approach, with highest weight assigned to 7.7 (Frankel *et al*., 2002; Petersen *et al*., 2008).

Investigation of the Charleston earthquake dates back to the immediate post-earthquake investigations led by Clarence Dutton, an Army officer detailed to the U.S. Geological Survey. This effort culminated in the publication of one of the earliest comprehensive, scientific reports of a large earthquake (Dutton, 1889). The so-called Dutton Report includes thorough and consistent compilations of near-field geological effects of the earthquake and accounts of far-field macroseismic effects. Whereas about 100 or fewer intensity values are available for each of the New Madrid mainshocks, the Dutton Report provides the basis for assignment of over 1,000 intensity values. In a comprehensive interpretation of these accounts, Bollinger (1977) assigned almost 800 intensity values based on the 1,337 intensity reports tallied by Dutton (1889). Bollinger (1977) estimated an m_b value of 6.8–7.1

using the same techniques that Nuttli (1973a, b) used to estimate magnitudes for the New Madrid earthquakes. The intensity values determined by Bollinger (1977) have provided the basis for later investigation using increasingly modern methodology. Johnston (1996) estimated M_w 7.3 +/− 0.26 for the Charleston earthquake. Bakun and Hopper (2004) report a preferred M_w value of 6.9. Published M_w values for the Charleston earthquake have thus been relatively consistent: the U.S. National Hazards Mapping project currently assumes a range between M 6.8 and 7.5, with highest weight given to a value of 7.3 (Frankel *et al*., 2002).

Comparing the intensity distributions of the 1886 mainshock with the best characterized intensity distribution from the 1811–1812 New Madrid sequence (the December mainshock), Hough (2004) concludes that these events had comparable magnitudes. Based on the results of Hough and Page (2011), this suggests $M_w \approx 6.8$ for the Charleston mainshock, consistent with the estimate of Bakun and Hopper (2004). This estimate is also consistent with the results of Leon *et al*. (2005), who analyze liquefaction observations and estimate magnitudes of Charleston paleoearthquakes of 6.5–7.0.

12.2.3 Historical earthquakes: recurrence rates

To estimate the seismic moment release rates for the NMSZ and CHSZ, it is necessary to estimate both the size of the large historical events, which are assumed to be characteristic earthquakes for their respective source zones, and their average recurrence rates. Sand blows generated by prehistoric earthquakes have been identified in both the NMSZ and Charleston regions. Although it is likely that future investigations will improve estimates of recurrence times, studies to date have produced compelling evidence of prehistoric earthquakes comparable in magnitude to those in historic times. Paleoseismic investigations suggest a repeat time on the order of 400–500 years over the past 2,000–3,000 years for both the New Madrid sequence and the Charleston earthquake (Talwani and Cox, 1985; Talwani and Schaeffer, 2001; Tuttle *et al*., 2002); they also suggest that the NMSZ tends to produce prolonged sequences with multiple, distinct mainshocks, the magnitudes of which are comparable to those of the 1811–1812 events (e.g., Tuttle and Schweig, 1996; Tuttle *et al*., 2002).

As summarized by Grollimund and Zoback (2001), this documented rate of Holocene NMSZ activity cannot be representative of a long-term rate (e.g., Schweig and Ellis, 1994), because extensive seismic reflection data reveal small cumulative offsets in post-Cretaceous embayment sediments (e.g., Hamilton and Zoback, 1981). Van Arsdale (2000) concluded from a combination of trench and reflection results that Holocene slip rates on the Reelfoot fault are at least four orders of magnitude higher than during the Pleistocene. Pratt (2012) suggests that pre-Holocene seismic activity involved faults other than those currently active in the NMSZ. However, in all attempts to model NMSZ seismogenesis, including that of Grollimund and Zoback (2001), it is taken as an incontrovertible constraint that NMSZ activity has "turned on" at some point in the relatively recent geological past, most likely within the Holocene.

12.2.4 Prehistoric earthquakes in other regions

Paleoseismic investigations in the CEUS have generally focused in the regions where large earthquakes occurred during historical times. However, paleoliquefaction features have been identified in other places in the CEUS, away from the NMSZ and the CHSZ. Significant paleoliquefaction features have been documented in the Wabash Valley (e.g., Munson *et al*., 1997) associated with a large earthquake approximately 6,100 years BP. Green *et al*. (2004) reassessed the magnitude of this event, known as the Vincennes earthquake, using recently developed field and analytical techniques, estimating an approximate magnitude of M_w 7.5. The results of these investigations have been incorporated in the USGS hazard map. The Wabash Valley remains seismically active in modern times: since 1900 the region has produced a higher rate of $M \geq 5$ events than the NMSZ, which has not produced an earthquake larger than M 5 since 1895.

More recently, Al-Shukri *et al*. (2005) documented evidence for a significant paleoliquefaction feature near Marianna, Arkansas, more than 100 km south of the currently seismically active segments of the NMSZ. These sand blows, dated to approximately 5,500 years BP, have very large dimensions, comparable to those found in the NMSZ. As noted by Tuttle *et al*. (2006), initial findings from the Marianna site suggest that seismicity might vary in space and time within the Reelfoot fault system (i.e., beyond the NMSZ proper), although more field investigation is needed to assess the history of activity at the Marianna site. Additionally, a number of geological investigations, including seismic reflection profiling and trenching, within or adjacent to the greater NMSZ have pointed towards Holocene activity on faults other than those apparently involved with the 1811–1812 sequence (e.g., Cox *et al*., 2001; Magnani *et al*., 2011). Several studies have presented evidence for Holocene faulting along the Commerce Geophysical lineament, which trends northeastward through central Arkansas, southeastern Missouri, southern Illinois, and south/central Indiana (Baldwin *et al*., 2006; Harrison *et al*., 1999; Figure 12.4). Conceivably, further investigation of Holocene faults adjacent to the central NMSZ could provide additional evidence for localized hazard, but without magnitude estimates or recurrence rates it is impossible to predict the implications for hazard.

Recent NSHMP maps assume a characteristic earthquake distribution for the NMSZ and the CHSZ; i.e., the rate of large events estimated from paleoseismic evidence is significantly higher than an extrapolation of background seismicity rates assuming a Gutenberg–Richter distribution (Gutenberg and Richter, 1944). (For the NMSZ, the rate of characteristic events is higher than the extrapolated Gutenberg–Richter rate by a factor of $\sim$3 to a factor of 10 or more, depending on the assumed magnitude of the characteristic earthquakes [see Stein and Newman, 2004]). Apart from these two source zones and the Cheraw and Meers faults in Colorado and Oklahoma, respectively, earthquake rates for the United States national seismic hazard maps are estimated from background seismicity rates assuming a Gutenberg–Richter distribution, with an imposed M_{max} of 7.5 in rifted crust and 7.0 in SCR regions apart from rift zones (e.g., Frankel *et al*., 2002).

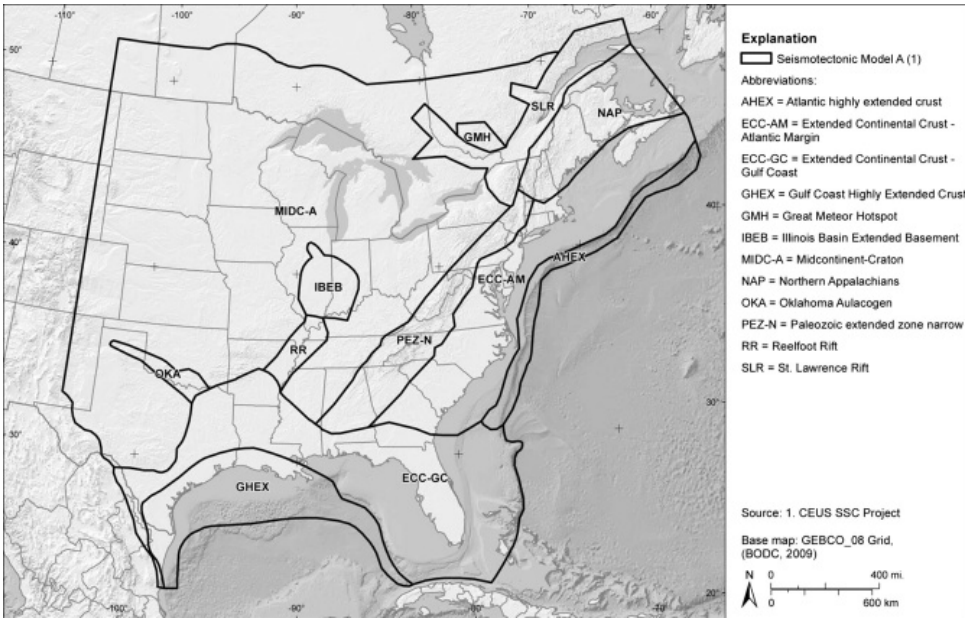

Figure 12.4 Seismotectonic zonation map developed for CEUS–SSC project (modified from Coppersmith *et al*., 2012). The aim of this project was not to identify all failed rifts within the mid-continent region, but only those considered to have an elevated earthquake potential relative to stable continental regions. The Commerce Geophysical Lineament tracks the northwestern edge of the Reelfoot Rift (RR), extending from roughly the southwestern corner of the RR, continuing through the Illinois Basin Extended Basin (IBEB).

12.3 Strain rate

12.3.1 Observed strain rate

The interiors of tectonic plates are assumed to be rigid, with strain rates 3–4 orders of magnitude lower than active plate boundaries. In the NMSZ, increasingly precise estimates of strain rate from GPS data have revealed an increasingly tight upper bound on the level of strain accrual in the region. Although the initial investigation of Liu *et al*. (1992) estimated a strain rate of 5–7 mm/yr across the Reelfoot fault based on a combination of GPS data and triangulation data dating back to the 1950s, Calais *et al*. (2005) show that no statistically significant site motions are found within the NMSZ using GPS data collected through 2005. Using GPS data recorded through 2005, Calais *et al*. (2005) estimate an upper bound on residual velocities relative to stable North America of 1.4 mm/yr, at a 95% confidence level. Frankel *et al*. (2012) analyze GPS data recorded through 2010 and conclude that there is statistically significant motion of 0.37 +/− 0.07 mm/yr across the Reelfoot fault at the surface, which they show is consistent with an interseismic deep creep rate of 4 mm/yr on the Reelfoot fault at depths between 12 and 20 km. Their model predicts that sufficient strain will accumulate across the zone to produce a $M_w \approx 7.3$ earthquake every 500 years, which

is roughly consistent with the Holocene paleoseismic record if characteristic earthquakes are low magnitude 7.

Any model derived from surface measurements of strain is non-unique, with generally poor resolution at depth (e.g., Page *et al*., 2009). The assumed rupture length for a Reelfoot fault event is moreover uncertain. To estimate a magnitude for a Reelfoot fault event, Frankel *et al*. (2012) assume a rupture length of 60 km, with rupture extending over a full 24 km down-dip width. This rupture length is based primarily on the distribution of present-day microseismicity. Based on analog and box modeling, Pratt (2012) concludes that thrust faulting does extend over the full length of the central NMSZ limb as defined by microseismicity (see Figure 12.3.) However, as noted earlier, several other lines of evidence suggest predominant moment release associated with NM3 involved a shorter rupture length, bounded between the intersections of the Reelfoot and the northern and southern limbs of the NMSZ (Figure 12.3): (1) an extension of thrust motion south/southeast of the intersection of the Cottonwood Grove and Reelfoot faults is kinematically inconsistent, as right-lateral strike-slip movement on the Cottonwood Grove fault would lower the likelihood of failure of the thrust fault extending south/southeast of the junction with the Reelfoot fault (e.g., Mueller *et al*., 2004); (2) the scarp/surface flexure associated with the Reelfoot fault is less well expressed geomorphically to the south/southeast of the intersection (e.g., Champion *et al*., 2001); (3) Mueller *et al*. (2004) show that the "side limbs" on the NMSZ are consistent with off-fault lobes of increased Coulomb stress generated by ruptures on two master faults, the Cottonwood Grove and Reelfoot faults. Further, it is possible that the southeastern extension of the Reelfoot fault ruptured not during the February mainshock but rather during the dawn aftershock (NM1-A), as proposed by Hough and Martin (2002). Thus, while a plausible case can be made for a longer rupture length, a length of 40 km is also defensible. If one assumes a rupture length of 40 km and a depth of 20 km, the moment of a "500-year event" inferred by Frankel *et al*. (2012) would be reduced by nearly a factor of 2 (i.e., the ratio of fault area: 800 km^2/1440 km^2), implying a M_w of 7.1 rather than 7.3. It has sometimes been suggested that the magnitudes of the 1811–1812 earthquakes could be higher than predicted from standard scaling relationships by virtue of high stress drop and/or unusually high shear modulus (e.g., Johnston, 1996). However, as discussed by Hanks and Johnston (1992), there is a strong dependence of high-frequency strong ground motions on stress drop. It is thus not possible to appeal to high stress drop as an explanation for high magnitudes, if the magnitudes are determined from high-frequency ground motions (i.e., intensities). In fact Hanks and Johnston (1992) themselves conclude that both the 1811–1812 mainshocks and the 1886 Charleston earthquake might be "no larger than $M = 6.5$ to 7, provided their stress drops are higher than average by a factor of 2 or so." (Note that this estimate was based on the original intensity assignments for the 1811–1812 earthquakes.)

The strain-rate observations from the NMSZ are thus consistent with two interpretations: (1) As argued by Hough and Page (2011), and corroborated by Frankel *et al*. (2012), a localized low but non-zero surface strain rate (e.g., 10^{-9}/yr), within the bounds imposed by the most recent GPS studies, could be sufficient to account for a sequence with an equivalent

$M_w \approx 7$ event every 500 years, a rate that is roughly consistent with the historic and prehistoric moment release rate if the principal 1811–1812 events and earlier mainshocks were in the range M_w 6.7–7; or (2) the principal 1811–1812 events were significantly larger than M_w 7, in which case deep-seated strain accrual processes in the NMSZ give rise to very low rates of surface deformation that are close to the level of detectability with available GPS data (e.g., see Kenner and Segall, 2000). The latter interpretation could be effectively untestable, at least in the foreseeable future, although increasingly precise results from GPS data will continue to improve an upper bound on strain accrual. I suggest the former interpretation is more likely, and better supported by available evidence.

12.3.2 Mechanism of strain accrual

The mechanism for localized strain accumulation in the NMSZ further remains enigmatic. Several mechanisms have been proposed, including (1) stress concentration associated with a Paleozoic mafic rift pillow (Grana and Richardson, 1996; Stuart *et al*., 1997); (2) glacial isostatic adjustment (GIA) following the removal of the Laurentide ice sheet (e.g., Grollimund and Zoback, 2001); (3) localized mantle flow driven by descent of the ancient Farallon slab (e.g., Forte *et al*., 2007); and (4) isostatic adjustment following the rapid incision of the Mississippi River Valley (Van Arsdale *et al*., 2007; Calais *et al*., 2011). As discussed by Talwani (this volume), the predicted magnitudes of stresses generated by the second and fourth mechanisms are low, which poses a problem for appealing to these mechanisms as the explanation for Holocene NMSZ activity. However, the explanations are attractive because they provide a qualitative and to some extent quantitative explanation for why NMSZ activity has been concentrated in the late Holocene (e.g., Kelson *et al*., 1996; Tuttle *et al*., 2002). There is no question that GIA contributes a significant level of present-day strain in eastern North America, not only over the region formerly covered by the Laurentide ice sheet but also well to the south, in the forebulge region (e.g., James and Bent, 1994; Grollimund and Zoback, 2001). Glacial isostatic adjustment is sometimes discounted as the likely cause of seismic activity because the strain signal is spatially distributed whereas significant moment release is apparently localized. Also, Wu and Johnston (2000) discounted the importance of the mechanism for NMSZ activity because earthquakes triggered by GIA in this location are predicted to have predominantly thrust mechanisms. However, unlike earlier interpretations of the 1811–1812 sequence (e.g., Johnston, 1996), the sequence is characterized by a predominantly thrust mechanism in the interpretations of Hough *et al*. (2000) and Hough and Page (2011). It is moreover plausible that GIA is a necessary but not sufficient condition for seismic activity: it has long been proposed that pre-existing zones of weakness such as failed rifts concentrate strain in intraplate crust (e.g., Sykes, 1978). Along the St. Lawrence Seaway in Canada, where the present-day GIA signal is higher than in the New Madrid region and has been measured with GPS data, Mazzotti *et al*. (2005) show that Holocene seismic moment release is consistent with the strain accrual associated with GIA (within the limitations of the short historical earthquake catalog).

Although the association of elevated modern-day seismicity with failed rifts dates back to the earliest efforts to develop models for CEUS (and intraplate) seismogenesis, some key questions clearly remain unanswered. For example, the Precambrian Mid-Continent (Keweenawan) Rift (e.g., Keller *et al*., 1983) through the upper Midwest has not been characterized by elevated seismicity during the instrumental era. One possibility is that GIA and the presence of a failed rift together are a necessary but not a sufficient condition for elevated activity. Another possibility is that, as I discuss more in a later section, the historical catalog is simply too short to reveal all active source zones if recurrence intervals are long. I note, for example, that the largest historical earthquake in the state of Nebraska, an estimated M 5.1 event on November 15, 1877, is inferred to be associated with the western flank of the Keweenan mafic belt; it is possible, given the uncertainties in the event location, that this event was within the rift.

12.3.3 Distributed strain release: a simple model

I now explore simple calculations to consider the possibility that CEUS moment release is driven by strain accrual that is low but more spatially distributed than current hazard maps suggest. The precise level of strain rate is unknown. Although attempts have been made to estimate strain rates from historical moment release rates (e.g., Anderson, 1986), these are not expected to be reliable given the short catalog and the enormous uncertainties associated with the magnitude estimates of the largest events. Somewhat better constraint is available from GPS investigations. Calais *et al*. (2011) estimate only an upper bound of 1.3×10^{-9}/yr in the NMSZ, while Galgana and Hamburger (2011) recently estimated a value of 1–2 $\times 10^{-9}$/yr in the Wabash valley. The model of Grollimund and Zoback (2001), which includes an imposed zone of weakness centered on the NMSZ, predicts a strain rate from GIA on the order of 10^{-9}/yr.

As an initial conservative estimate, I assume a strain rate of 0.5–1.0 $\times 10^{-9}$/yr is distributed over the failed rifts that have elevated seismic potential (Coppersmith *et al*., 2012), and that these zones cumulatively make up approximately 10% of the CEUS–SCR crust (Figure 12.4). A moment rate corresponding to distributed strain accumulation can be estimated from

$$d\varepsilon/dt = dM_o/dt/(2.67\mu \mathrm{Ah}) \tag{12.1}$$

where h is the thickness of the brittle layer, μ is shear modulus taken to be 3×10^{11} dyne/cm^2, and A is area (Anderson, 1986). As an illustrative simple calculation, I consider a total CEUS area of 2800 $\times$ 2400 km^2 in which there is an elevated strain rate of 0.5–1.0 $\times 10^{-9}$ within failed rifts that make up 10% of the total area. Assuming $h = 15$ and no aseismic strain release, Equation (12.1) predicts an overall moment accrual rate of (4–8) $\times 10^{24}$ dyne cm/yr. If this rate were released solely in M_{max} events, it would be sufficient to produce one M_w 7.0 earthquake somewhere within failed rifts every 45–90 years. Assuming that 10% of the moment rate is released by smaller earthquakes, the result is 50–100 years. Further

assuming a *b*-value of 1, this corresponds to a M_w 6 or greater earthquake approximately one every 5–10 years.

The above calculation, while highly simplified, can be compared with the observed rate of large earthquakes in the CEUS. The rate of $M_w \geq 7$ events is difficult to estimate, so I instead consider the rate of $M_w \approx 6$ events. For example, since 1850 there have been approximately six CEUS earthquakes with magnitudes close to M_w 6, as well as the 1886 mainshock: the largest aftershock of the 1886 Charleston earthquake (Talwani and Sharma, 1999), the 1895 Charleston, MO, earthquake (Bakun and Hopper, 2004), the 1897 Giles County, VA, earthquake (Bollinger and Hopper, 1971), the 1931 Valentine, TX, earthquake (Doser, 1987), the 1944 Massena, NY, earthquake (Bent, 1996), and the 2011 Mineral, VA, earthquake (e.g., http://neic.usgs.gov/neis/eq_depot/2011/eq_110823_se082311a/se082311a_l.html, last accessed 19 Dec. 2012). The observed rate of $M_w \geq 6$ events between 1850 and 2013 has thus been one every 23 years, an obviously rough estimate of long-term rate but one that is within a factor of 2–4 of the ballpark estimate. If one instead considers the expected rate of $M_w \geq 5.8$ events based on the above model, since several of the historical earthquakes were slightly smaller than M_w 6, the expected rate is higher (one every 3–6 years) than the ballpark estimate. I note, however, that (1) the discrepancy is significantly smaller than any model that proposes to account for $M_w \geq 7.5$ earthquakes every ~500 years given best-available constraints on strain rate, and (2) both the calculation and the estimation of observed rates are highly simplified and uncertain. For example, the list of observed earthquakes since 1850 excludes five events that occurred in Canada but within the region defined in Figure 12.4. Other complications abound. For example, as shown by Hough *et al*. (2003), even a low level of permanent deformation (e.g., folding, or pressure solution) could account for a higher percentage of overall strain release in a low strain rate region than an active plate boundary, reducing the level of strain released seismically. For example, using calculations based on a simple model, they show that, for a strain rate of 5×10^{-8}/yr, permanent deformation will reduce accrued strain on the order of 30% over 3,000 years. For this and other reasons, a quantitative assessment of strain accrual is highly uncertain. The key point, however, is that even a low level of distributed strain accrual can generate a significant (and distributed) overall hazard. That is, even a strain rate as low as 0.5×10^{-9}/yr would be sufficient to produce as many or more large earthquakes as have been observed in historical times, if the strain is distributed over a region covering roughly 10% of the CEUS. (While significant non-zero strain rates have only barely been observed to-date in the NMSZ and Wabash region, a rate on the order of 0.5×10^{-9}/yr would be below the current level of detection in other CEUS regions.)

12.3.4 Other intraplate regions

A growing body of geological evidence reveals that many faults in low strain rate regions generate large earthquakes that are clustered on timescales of a few centuries to perhaps a few millennia, with much longer intervening periods when the fault might be considered

dormant. Examples (see Coppersmith [1988] and Crone *et al*. [2003] for summaries) include the Meers fault in Oklahoma (Crone and Luza, 1990), the clear scarp of which is inferred to have been generated by two M ≈ 7 earthquakes during the past ~3,000 years, with no evidence of prior events over 100,000 years or more (see Crone *et al*., 2003), and the Cheraw fault in Colorado, which has produced three large earthquakes between 8 and 25 ka BP.

Especially compelling geological evidence for temporally clustered seismic activity on individual faults has been documented in Australia. A number of active faults in Australia reveal behavior similar to that of the Meers fault (e.g., Crone *et al*., 2003; Clark *et al*., 2012), including the Roopena fault in South Australia, the Hyden fault in Western Australia, and the Lake Edgar fault in southwest Tasmania. To quote Clark *et al*. (2012), "A common characteristic of morphogenic earthquake activity in Australia appears to be temporal clustering. Periods of earthquake activity comprising a finite number of large events are separated by much longer periods of seismic quiescence." In eastern Utah, in a region east of the Basin and Range province, where a precise strain rate estimate is not available but thought to be low, Schwartz *et al*. (2012) summarize evidence that the entire neotectonic history of the Bear River fault consists of two M 6–6.5 surface-rupturing normal earthquakes during the late Holocene.

In low strain rate regions of China, the especially long historical record reveals that large earthquakes have occurred throughout a broad region, with no evidence for clustering or even repeated large events in any individual source zone over the past ~700 years (Liu *et al*., 2011). One key caveat is that paleoseismological investigations that might document recurrence intervals have apparently not been undertaken at the source zones discussed by Liu *et al*. (2011). However, with a historical record extending back to 1300, it is unlikely that individual source zones in low strain rate regions in China are characterized by the same type of clustering documented in the NMSZ and CHSZ. It is not clear why low strain rate regions in China do not (apparently) generate the same type of clustering that appears to be common in other regions.

One possible explanation for clustering is a feedback mechanism between an effectively embedded finite fault in the upper crust and a viscoelastic lower crust (e.g., Kenner and Segall, 2000). In such a setting, an initial episode of strain release can trigger a sequence of large events as post-seismic motions in a deep viscoelastic layer repeatedly reload an individual fault in the brittle crust. A simplified analytical model predicts that the recurrence interval will scale linearly with the viscosity of the weak lower crust (Kenner and Segall, 2000). One might conjecture, then, that differences in degree of clustering in different regions are due to differences in lower crustal viscosity. Lower crustal viscosity is poorly constrained on a global basis. However, absolute plate motions are well established, and are known to vary significantly among intraplate regions (Table 12.1.) It has been shown that plate motions are driven primarily by lateral forces (e.g., Forsyth and Uyeda, 1975; Conrad and Lithgow-Bertelloni, 2002), but drag on the bottom of plates influences plate motion as well, and is stronger under continents than oceans (Forsyth and Uyeda, 1975). A relatively fast plate motion might therefore be expected to correlate to some extent

Table 12.1 *Plate rate versus propensity for large event clustering for four tectonic plates*

Tectonic plate	Plate rate (cm/yr)	Short-term clustering?
Australian	5.8	Yes
Indian	2.6	No?
North American	4.1	Yes
Eurasian	2.3	No

with low viscosity and, therefore, with a shorter recurrence interval for individual source zones. This hypothesis is highly speculative; however, both Australia and North America are characterized by relatively fast plate rates and clustering, whereas peninsular India and Eurasia are characterized by significantly lower plate rates and no clustering.

In any case, in all of the intraplate regions discussed above, evidence points to earthquake activity that in some SCR regions tends to be clustered on timescales of centuries to a few millennia, and that in all SCR regions is distributed throughout a broad region over longer timescales.

12.4 Statistical considerations

In the absence of geological and geodetic constraints on fault slip rates or direct evidence for large characteristic earthquakes, PSHA calculations have long relied on the observed rate of small-to-moderate earthquakes in a region to estimate the expected rate of large earthquakes. This practice is motivated by good evidence that, through any given region, seismicity is characterized by a Gutenberg–Richter magnitude distribution (Gutenberg and Richter, 1944) with a *b*-value of 1.0 (e.g., King, 1983; Felzer, 2006). The practice is further justified by appealing to the assumption of stationarity; the same rationale is sometimes also used to estimate M_{max}. However, it has been shown that a stationary process, for example the Epistemic Triggering of Aftershock (ETAS) model (Kagan and Knopoff, 1981; Ogata, 1988), will give rise to a constant *b*-value but an apparent *a*-value that can vary considerably if estimated from a relatively short earthquake catalog (Page *et al*., 2010). As shown by Stein and Newman (2004), within a short catalog large earthquakes can appear to be either characteristic or "uncharacteristic"; i.e., to not be represented in the catalog at the average long-term rate.

The ETAS model, which provides an integrated framework for seismicity including foreshock and aftershock probabilities, has been shown to match the degree of clustering observed in typical earthquake catalogs (e.g., Hardebeck *et al*., 2008). An ETAS model predicts not only traditional foreshock/aftershock clustering, but also regional clustering of moderate earthquakes. In California, for example, such clustering can give rise to periods of

relative high or low activity that extend for several decades (Hardebeck *et al*., 2008). Using simulated ETAS catalogs, Page *et al*. (2010) show that, for any region, reliable estimation of a long-term *a*-value requires a catalog that is several times longer than the recurrence time of the M_{max} event in the region. Even in California, where strain rate is relatively high, the long-term *a*-value remains uncertain by 20% or more (e.g., WGCEP, 2013). Relative to California, the historical record in the CEUS is at most a factor of 2 longer, but the strain rate is a factor of 1,000 or more lower. Even without detailed statistical calculations, it is clear that a 100- or 300-year snapshot of seismicity cannot capture all potentially active source zones or provide a reliable estimate of long-term rates on timescales of millennia.

12.5 Discussion and conclusions

Quantification of seismic hazard in the CEUS, and by extension any similar low strain rate region, emerges as a daunting prospect. Probabilistic seismic hazard assessment remains challenging in a well-studied, high strain rate region such as California (e.g., WGCEP, 2013), where geological and geodetic constraints are each uncertain, but presumably allow hazard to be characterized to first order. In the low strain rate CEUS region, where the seismic catalog is at best a factor of 2–10 longer than that in California, earthquake rates are a factor of 1,000 or more lower, geological and geodetic constraints are limited or non-existent, and hazard is likely to be dominated by low-probability events. There is little question that the inputs, for example given published magnitude estimates of characteristic earthquakes that vary by nearly a full magnitude unit, to PSHA remain highly uncertain in a low strain rate region. And, again, to quote from Clark *et al*. (2012), "This apparent bimodal recurrence behavior poses challenges for probabilistic seismic hazard assessment."

In the absence of adequate constraint on long-term slip rates, deformation, and seismic rates, an alternative to the use of smoothed seismicity models involves consideration of tectonic zonation. Since 2005 the seismic hazard map of Canada has been determined in part based on an interpretation of tectonic zonation (e.g., Adams and Halchuk, 2003). Whereas the maps prior to 2005 had conspicuous "bull's-eyes" around the largest known late Holocene earthquakes, high hazard in the new maps is more distributed throughout broader zones, with less pronounced bull's-eyes corresponding to regions of historical activity.

As paleoseismologists continue to study the Central and Eastern United States, it also appears likely that geological investigations will identify other source zones that have produced large Holocene earthquakes. Inclusion of rates based on observed prehistoric earthquakes in other areas will likely serve to distribute hazard over broader zones. A reduction of the estimated magnitudes of the New Madrid and perhaps Charleston mainshocks would further serve to lessen the estimated hazard in proximity to these zones.

A fundamental challenge, however, will be to account for uncertainties associated with long-term rate estimates, not only in the NMSZ and CHSZ regions, but also in regions where no large earthquake has occurred during historical times. In the NMSZ and CHSZ, as

discussed earlier, late Holocene recurrence rates of large earthquakes have been estimated, but it is not clear whether recent events are part of (relatively) short-term clusters that will eventually end. For these regions there is a consensus if not a unanimous view that PSHA treatments should assume that future rates will be comparable to those estimated for recent millennia.

As pointed out by Stein and Newman (2004), short catalogs can give rise to not only apparent characteristic earthquakes with shorter recurrence rates than the long-term rate, but also to earthquakes that appear less frequently than their long-term rates ("uncharacteristic earthquakes.") The possibility has been at least discussed, for example at the 2012 National Seismic Hazard Mapping Program CEUS workshop, of including a low-weight branch in a logic-tree approach corresponding to the possibility that no large ($M > 7$) earthquakes will occur in the future in the NMSZ. One possible treatment of uncertainties associated with the short historical catalog and limited geological record, then, would also include logic-tree branches corresponding to the possibility that other source zones might produce large earthquakes at a higher rate over the next few millennia than the rate observed during the late Holocene.

Acknowledgments

I thank Pradeep Talwani for the invitation to contribute to this volume, as well as for feedback on the chapter, and am grateful to Oliver Boyd, Rob Williams, and an anonymous reviewer for critical reviews that improved the manuscript. I also acknowledge Karen Felzer and Morgan Page for many helpful discussions.

References

Adams, J., and Halchuk, S. (2003). *Fourth Generation Seismic Hazard Maps of Canada: Values for Over 650 Canadian Localities Intended for the 2005 National Building Code of Canada*. Geological Survey of Canada.

Al-Shukri, H. J., Lemmer, R. E., Mahdi, H. H., and Connelly, J. B. (2005). Spatial and temporal characteristics of paleoseismic features in the southern terminus of the New Madrid seismic zone in eastern Arkansas. *Seismological Research Letters*, 76, 502–511, doi:10.1785/gssrl.76.4.502.

Anderson, J. G. (1986). Seismic strain rates in the central and eastern United States. *Bulletin of the Seismological Society of America*, 76, 273–290.

Bakun, W. H., and Hopper, M. (2004). Magnitudes and locations of the 1811–1812 New Madrid, Missouri and the 1886 Charleston, South Carolina earthquakes. *Bulletin of the Seismological Society of America*, 94, 64–75.

Baldwin, J. N., Witter, R. C., Vaughn, J. D., *et al*. (2006). Geological characterization of the Idalia Hill fault zone and its structural association with the Commerce Geophysical Lineament, Idalia, Missouri. *Bulletin of the Seismological Society of America*, 96, 2281–230, doi: 10.1785/0120050136.

Bent, A. (1996). Source parameters of the damaging Cornwall-Massena earthquake of 1944 from regional waveforms. *Bulletin of the Seismological Society of America*, 86, 489–497.

Bollinger, G. A. (1977). Reinterpretation of the intensity data for the 1886 Charleston, South Carolina, earthquake. In *Studies Related to the Charleston, South Carolina Earthquake of 1886: A Preliminary Report*, ed. D. W. Rankin, U.S. Geological Survey Professional Paper 1028, pp. 17–32.

Bollinger, G. A., and Hopper, M. (1971). Virginia's two largest earthquakes – December 22, 1875 and May 31, 1897. *Bulletin of the Seismological Society of America*, 61, 1033–1039.

Calais, E., Han, J. Y., DeMets, C., and Nocquet, J. M. (2005). Deformation of the North American plate interior from a decade of continuous GPS measurements. *Journal of Geophysical Research*, 111, B06402, doi: 10.1029/2005JB004253.

Calais, E., Freed, A. M., Van Ardsale, R., and Stein, S. (2011). Triggering of New Madrid seismicity by late-Pleistocene erosion. *Nature*, 566, 608-U2, doi: 10.1038/nature09258.

Champion, J., Mueller, K., Tate, A., and Guccione, M. (2001). Geometry, numerical models and revised slip rate for the Reelfoot fault and trishear fault-propagation fold, New Madrid seismic zone. *Engineering Geology*, 62, 31–49, doi: 10.1016/S0013-7952(01)00048-5.

Clark, D., McPherson, A., and Van Dissen, R. (2012). The long-term behavior of the Australian stable continental region (SCR) faults. *Tectonophysics*, 566, 1–30, doi: 10.1016/j.tecto.2012.07.004.

Conrad, C. P., and Lithgow-Bertelloni, C. (2002). How mantle slabs drive plate tectonics. *Science*, 298, 207–209, doi: 10.1126/science.1074161.

Coppersmith, K. (1988). Temporal and spatial clustering of earthquake activity in the Central and Eastern United States. *Seismological Research Letters*, 59, 299–304, doi:10.1785/gssrl.59.4.299.

Coppersmith, K. J., Salomone, L. A., Fuller, C. W., *et al*. (2012). *Central and Eastern United States (CEUS) Seismic Source Characterization (SSC) for Nuclear Facilities Project* (No. DOE/NE-0140). Electric Power Research Institute.

Cox, R. T., Van Arsdale, R. B., Harris, J. B., and Larsen, D. (2001). Reelfoot rift zone margin, central United States, and implications for regional strain accumulation. *Geology*, 29, 419–422, doi: 10.1130/0091-7613(2001)029<0419:NOTSTRR>2.0.CO;2.

Crone, A. J., and Luza, K. V. (1990). Style and timing of Holocene surface faulting on the Meers fault, southwestern Oklahoma. *Geological Society of America Bulletin*, 102, 1–17, doi:10.1130/0016–7606(1990).

Crone, A. J., De Martini, P. M., Machette, M. N., Okumura, K., and Prescott, J. R. (2003). Quiescent faults in Australia: implications for fault behavior in stable continental regions. *Bulletin of the Seismological Society of America*, 93, 1913–1934, doi: 10.1785/010000094.

Doser, D. I. (1987). The 16 August 1931 Valentine, Texas, earthquake: evidence for normal faulting in west Texas. *Bulletin of the Seismological Society of America*, 77, 2005–2017.

Drake, D. (1815). *Natural and Statistical View, or Picture of Cincinnati and the Miami County, Illustrated by Maps*. Cincinnati: Looker and Wallace.

Dura-Gomez, I., and Talwani, P. (2009). Finding faults in the Charleston Area, South Carolina: 1. Seismological data. *Seismological Research Letters*, 80, 883–900, doi: 10.1785/gssrl.80.5.883.

Dutton, C. (1889). The Charleston earthquake of August 31, 1886. *U.S. Geological Survey Ninth Annual Report, 1887–88*, pp. 203–528.

Ebel, J. E., Bonjer, K.-P., and Oncescu, M. C. (2000). Paleoseismicity: seismicity evidence for past large earthquakes. *Seismological Research Letters*, 71, 283–294, doi: 10.1785/gssrl.71.2.283.

Felzer, K. R. (2006). Calculating the Gutenberg–Richter *b*-value (abstract), American Geophysical Union Fall meeting, abstract S42C-08.

Forsyth, D., and Uyeda, S. (1975). On the relative importance of the driving forces of plate motion. *Geophysical Journal of the Royal Astronomical Society*, 43, 163–200.

Forte, A. M., Mitrovica, J. X., Moucha, R., Simmons, N. A., and Grand, S. P. (2007). Descent of ancient Farallon slab drives localized flow below the New Madrid seismic zone. *Geophysical Research Letters*, 34, L04308, doi: 10.1029/2006GL027895.

Frankel, A., Petersen, M.D., Mueller, C. S., *et al*. (2002). Documentation for the 2002 Update of the National Seismic Hazard Maps. U.S. Geological Survey Open File Report 02-420.

Frankel, A., Smalley, R., and Paul, J. (2012). Significant motions between GPS sites in the New Madrid region: implications for seismic hazard. *Bulletin of the Seismological Society of America*, 102, 479–489. doi: 10.1785/0120100219.

Fuller, M. L. (1912). The New Madrid earthquakes. *U.S. Geological Survey Bulletin*, 494.

Galgana, G. A., and Hamburger, H. M. (2011). Geodetic observations of active intraplate crustal deformation in the Wabash Valley seismic zone and the southern Illinois basin. *Seismological Research Letters*, 81, 699–714, doi:10.1785/gssrl.81.5.699.

Gomberg, J. S. (1993). Tectonic deformation in the New Madrid seismic zone: inferences from map view and cross-sectional boundary element models. *Journal of Geophysical Research*, 98, 6639–6664.

Grana, J. P., and Richarson, R. M. (1996). Tectonic stress within the New Madrid seismic zone. *Journal of Geophysical Research*, 101, 5445–5458.

Green, R. A., Obermeier, S. F., and Olson, S. M. (2004). The role of paleoliquefaction studies in performance-based earthquake engineering in the central-eastern United States. 13th World Conference on Earthquake Engineering, Vancouver, Canada, August 1–6, Paper 1643.

Grollimund, B., and Zoback, M. D. (2001). Did glaciation trigger intraplate seismicity in the New Madrid Seismic Zone? *Geology*, 29, 175–178, doi:10.1130/0091–7613.

Gutenberg, B., and Richter, C. F. (1944). Frequency of earthquakes in California. *Bulletin of the Seismological Society of America*, 34, 185–188.

Hamilton, R. M., and Zoback, M. D. (1981). Tectonic features of the New Madrid seismic zone from seismic reflection profiles. In *Investigations of the New Madrid Earthquake Region*, ed. F. A. McKeown and L. C. Pakiser, U.S. Geological Survey Professional Paper 1236, pp. 55–82.

Hanks, T. C., and Johnston, A. C. (1992). Common features of the excitation and propagation of strong ground motion for North American earthquakes. *Bulletin of the Seismological Society of America*, 82, 1–23.

Hardebeck, J. L., Felzer, K. R., and Michael, A. J. (2008). Improved tests reveal that the accelerating moment release hypothesis is statistically insignificant. *Journal of Geophysical Research*, 113, B08310, doi:10.1029/2007JB005410.

Harrison, R. W., Hoffman, D., Vaughn, J. D., *et al*. (1999). An example of neotectonism in a continental interior: Thebes Gap, midcontinent, United States. *Tectonophysics*, 305, 399–417.

Holzer, T. L., Noce, T. E., and Burnett, M. J. (2011). Implications of liquefaction caused by the 1811–1812 New Madrid earthquakes for estimates of ground shaking and earthquake magnitudes (abstract). *Seismological Research Letters*, 82, 274.

Hough, S. E. (1996). The case against huge earthquakes. *Seismological Research Letters*, 67, 3–4.
Hough, S. E. (2001). Triggered earthquakes and the 1811–1812 New Madrid, central United States, earthquake sequence. *Bulletin of the Seismological Society of America*, 91, 1574–1581.
Hough, S. E. (2004). Scientific overview and historical context of the 1811–1812 New Madrid earthquake sequence. *Annals of Geophysics*, 47, 523–537.
Hough, S. E. (2009). Cataloging the 1811–1812 New Madrid, Central U.S. earthquake sequence. *Seismological Research Letters*, 80, 1045–1053.
Hough, S. E., and Martin, S. (2002). Magnitude estimates of two large aftershocks of the 16 December, 1811 New Madrid earthquake. *Bulletin of the Seismological Society of America*, 92, 3259–3268.
Hough, S. E., and Page, M. (2011). Towards a consistent model for strain accrual and release for the New Madrid Seismic Zone. *Journal of Geophysical Research*, 116, doi: 10.1029/2010JB007783.
Hough, S. E. (2013). Spatial variability of "Did You Feel It?" intensity data: insights into sampling biases in historical earthquake intensity distributions. *Bulletin of the Seismological Society of America*, 103, 2767– 2781.
Hough, S. E., Armbruster, J. G., Seeber, L., and Hough, J. F. (2000). On the modified Mercalli intensities and magnitudes of the 1811–1812 New Madrid, Central United States earthquakes. *Journal of Geophysical Research*, 105, 23, 839–823, 864.
Hough, S. E., Seeber, L., and Armbruster, J. G. (2003). Intraplate triggered earthquakes: observations and interpretation. *Bulletin of the Seismological Society of America*, 93, 2212–2221.
Hough, S. E., Bilham, R., Mueller, K., *et al*. (2005). Wagon loads of sand blows in White County, Illinois. *Seismological Research Letters*, 76, 373–386.
James, T. S., and Bent, A. L. (1994). A comparison of North American seismic strain rates to glacial rebound strain-rates. *Geophysical Research Letters*, 21, 2127–2130.
Johnston, A. C. (1996). Seismic moment assessment of earthquakes in stable continental regions III, New Madrid 1811–1812, Charleston 1886, and Lisbon 1755. *Geophysical Journal International*, 126, 314–344.
Johnston, A. C., and Schweig, E. S. (1996). The enigma of the New Madrid earthquakes of 1811–1812. *Annual Review of Earth and Planetary Science*, 24, 339–384, doi:10.1146/annurev.earth.24.1.339.
Kagan, Y. Y., and Knopoff, L. (1981). Stochastic synthesis of earthquake catalogs. *Journal of Geophysical Research*, 86, 2853–2862.
Keller, G. R., Lidiak, E. G., Hinze, W. J., and Braile, L. W. (1983). The role of rifting in the tectonic development of the midcontinent, U.S.A. *Tectonophysics*, 94, 391–412, doi:10.1016/0040-1951(83)90026-4.
Kelson, K. I., Simpson, G. D., VanArsdale, R. B., Haraden, C. C., and Lettis, W. R. (1996). Multiple late Holocene earthquakes along the Reelfoot fault, central New Madrid seismic zone. *Journal of Geophysical Research*, 101, 6151, doi: 10.1029/95JB01815.
Kenner, S. J., and Segall, P. (2000). A mechanical model for interplate earthquakes: application to the New Madrid Seismic Zone. *Science*, 289, 2329–2332.
King, G. (1983). The accommodation of large strains in the upper lithosphere of the earth and other solids by self-similar fault systems: the geometrical origin of *b*-value. *Pure and Applied Geophysics*, 121, 761–815.
Leon, E., Gassman, S. L., and Talwani, P. (2005). Effect of soil aging on assessing magnitudes and accelerations of prehistoric earthquakes. *Earthquake Spectra*, 21, 737–759.

Liu, L., Zoback, M.D., and Segall, P. (1992). Rapid intraplate strain accumulation in the New Madrid Seismic Zone. *Science*, 257, 1666–1669.

Liu, M., Stein, S., and Wang, H. (2011). 2000 years of migrating earthquakes in north China: how earthquakes in midcontinents differ from those at plate boundaries. *Lithosphere*, 3, 128–132, doi:10.1130/L129.1.

Magnani, M., McIntosh, K. D., and Guo, L. (2011). Paleotectonic control on distribution of long-term deformation in the central United States from high-resolution seismic data. Abstract S22A-03, American Geophysical Union Fall Meeting, San Francisco, CA.

Mazzotti, S., James, T. S., Henton, J., and Adams, J. (2005). GPS crustal strain, postglacial rebound, and seismic hazard in eastern North America: the Saint Lawrence valley example. *Journal of Geophysical Research*, 110, B11301, doi:10.1029/2004JB003590.

McMurtrie, H. (1819). *Sketches of Louisville and Its Environs; Including, Among a Great Miscellaneous Matter, a Florula Louisvillensis; or, a Catalogue of Nearly 400 Genera and 600 Species of Plants, That Grow in the Vicinity of the Town, Exhibiting Their Generic, Specific, and Vulgar English Names*. S. Penn, Jun. Main-street, Louisville.

Mitchill, S. L. (1815). A detailed narrative of the earthquakes which occurred on the 16th day of December, 1811. *Transactions of the Literary and Philosophical Society of New York*, 1, 281–307.

Mueller, K., Hough, S. E., and Bilham, R. (2004). Analysing the 1811–1812 New Madrid earthquakes with recent instrumentally recorded aftershocks. *Nature*, 429, 284–288.

Munson, P. J., Obermeier, S. F., Munson, C. A., and Hajic, M. R. (1997). Liquefaction evidence for Holocene and latest Pleistocene seismicity in the southern halves of Indiana and Illinois: a preliminary overview. *Seismological Research Letters*, 68, 521–536.

Newman, A., Stein, S., Weber, J., *et al.* (1999). Slow deformation and lower seismic hazard at the New Madrid seismic zone. *Science*, 284, 619–621.

Nuttli, O. W. (1973a). Seismic wave attenuation and magnitude relations for eastern North America. *Journal of Geophysical Research*, 78, 876, doi:10.1029/JB078i005p00876.

Nuttli, O. W. (1973b). The Mississippi Valley earthquakes of 1811 and 1812: intensities, ground motion, and magnitudes. *Bulletin of the Seismological Society of America*, 63, 227–248.

Nuttli, O. W. (1979). Seismicity of the central United States. *Geological Society of America, Reviews in Engineering Geology*, IV, 67–93.

Obermeier, S. F., Jacobson, R. B., Smoot, J. P., *et al.* (1990). Earthquake induced liquefaction features in the coastal setting of South Carolina and in the fluvial setting of the New Madrid Seismic Zone. U.S. Geological Survey Professional Paper 1504.

Odum, J. K., Stephenson, W. J., and Shedlock, K. M. (1998). Near-surface structural model for deformation associated with the February 7, 1812 New Madrid, Missouri, earthquake. *Geological Society of America Bulletin*, 110, 149–162.

Ogata, Y. (1988). Statistical models for earthquake occurrence and residual analysis for point processes. *Journal of the American Statistical Association*, 83, 9–27.

Omori, F. (1895). On the after-shocks of earthquakes. *Journal of the College of Science*, Imperial University of Tokyo, 7, 111–200.

Page, M. T., Custodio, S., Archuleta, R. J., and Carlson, J. M. (2009). Constraining earthquake source inversions with GPS data: 1. Resolution-based removal of artifacts. *Journal of Geophysical Research*, 114, B01314, doi:10.1029/2007JB005449.

Page, M., Felzer, K. R., Weldon, R. J., *et al.* (2010). The case for Gutenberg-Richter scaling on faults (abstract). *Seismological Research Letters*, 81, 330.

Page, M., Hough, S. E., and Felzer, K. (2012). Can current New Madrid seismicity be explained as a decaying aftershock sequence? Abstract S54D-07, American Geophysical Union Fall Meeting, San Francisco, CA, 3–7 December.

Petersen, M. D., Frankel, A. D., Harmsen, S.C., *et al*. (2008). *Documentation for the 2008 Update of the United States National Seismic Hazard Maps*. U.S. Geological Survey Open-File Report 2008–1128.

Pond, E. C., and Martin, J. R. (1997). Estimated magnitudes and accelerations associated with prehistoric earthquakes in the Wabash Valley region in the central U.S. *Seismological Research Letters*, 68, 611–623.

Pratt, T. L. (2012). Kinematics of the New Madrid seismic zone, central United States, based on stepover models. *Geology*, 40, 371–374, doi:10.1130/G32624.1.

Ramirez-Guzman, L., Graves, R. W., Olsen, K. B., *et al*. (2011a). Central United States earthquake ground motion simulation working group: the 1811–1812 New Madrid earthquake sequence (abstract). *Seismological Research Letters*, 82, 275.

Ramirez-Guzman, L., Graves, R. W., Olsen, K. B., *et al.* (2011b). Magnitude uncertainty and ground motion simulations of the 1811–1812 New Madrid earthquake sequence (abstract). American Geophysical Union Fall Meeting, abstract S22A-07.

Russ, D. P. (1982). Style and significance of surface deformation in the vicinity of New Madrid, Missouri. In *Investigations of the New Madrid Earthquake Region*, ed. F. A. McKeown and L. C. Pakiser, U.S. Geological Survey Professional Paper 1236, pp. 95–114.

Saucier, R. T. (1991). Geoarcheological evidence of strong prehistoric earthquakes in the New Madrid (Missouri) seismic zone. *Geology*, 19, 296–298, doi:10.1130/0091–7613(1991).

Schwartz, D. P., Hecker, S., Haproff, P., Beukelman, G., and Erickson, B. (2012). The Bear River fault zone, Wyoming and Utah: complex ruptures on a young normal fault (abstract). T31E-08, American Geophysical Union Fall Meeting.

Schweig, E. S., and Ellis, M. A. (1994). Reconciling short recurrence intervals with minor deformation in the New Madrid seismic zone. *Science*, 264, 1308–1311.

Seeber, L., and Armbruster, J. G. (1987). The 1886–1889 aftershocks of the Charleston, South Carolina, earthquake: a widespread burst of seismicity. *Journal of Geophysical Research*, 92, 2663–2696.

Stein, S., and Liu, M. (2009). Long aftershock sequences within continents and implications for earthquake hazard assessment. *Nature*, 462, doi: 10.1038/nature08502.

Stein, S., and Newman, A. (2004). Characteristic and uncharacteristic earthquakes as possible artifacts: application to the New Madrid and Wabash Valley seismic zones. *Seismological Research Letters*, 75, 173–198.

Street, R. (1982). A contribution to the documentation of the 1811–1812 Mississippi Valley earthquake sequence. *Earthquake Notes*, 53, 39–52.

Street, R. (1984). *The Historical Seismicity of the central United States: 1811–1928, Final Report*. Contract 14–08–0001–21251, Appendix A, Washington, D.C.: U.S. Geological Survey.

Stuart, W. D., Hildenbrand, T. G., and Simpson, R. W. (1997). Stressing of the New Madrid seismic zone by a lower crust detachment fault. *Journal of Geophysical Research*, 102, 27, 623–627, 633.

Sykes, L. R. (1978). Intra-plate seismicity, reactivation of preexisting zones of weakness, alkaline magmatism, and other tectonics post-dating continental separation. *Reviews of Geophysics and Space Physics*, 16, 621–688.

Talwani, P., and Cox, J. (1985). Paleoseismic evidence of recurrence of earthquakes near Charleston, South Carolina. *Science*, 229, 379–381, doi:10.1126/science.229/4711.379.

Talwani, P., and Dura-Gomez, I. (2009). Finding faults in the Charleston Area, South Carolina 2. Complementary data. *Seismological Research Letters*, 80, 901–919, doi:10.1785/gssrl.80.5.901.

Talwani, P., and Schaeffer, W. T. (2001). Reccurence rates of large earthquakes in the South Carolina Coastal Plain based on paleoliquefaction data. *Journal of Geophysical Research*, 106, 6621–6642.

Talwani, P., and Sharma, N. (1999). Reevaluation of the magnitude of three destructive aftershocks of the 1886 Charleston earthquake. *Seismological Research Letters*, 70, 360–367, doi:10.1785/gssrl.70.3.360.

Tuttle, M. P., and Schweig, E. S. (1996). Archaeological and pedological evidence for large prehistoric earthquakes in the New Madrid seismic zone, central United States. *Geology*, 23, 253–256.

Tuttle, M. P., Schweig, E. S., Sims, J. D., *et al*. (2002). The earthquake potential of the New Madrid seismic zone. *Bulletin of the Seismological Society of America*, 92, 2080–2089.

Tuttle, M. P., Al-Shukri, H., and Mahdi, H. (2006). Very large earthquakes centered southwest of the New Madrid seismic zone 5000–7000 years ago. *Seismological Research Letters*, 77, 755–770, doi:10.1785/gssrl.77.6.755.

Van Arsdale, R. (2000). Displacement history and slip rate on the Reelfoot fault of the New Madrid seismic zone. *Engineering Geology*, 55, 219–226.

Van Arsdale, R., Bresnahan, R., McCallister, N., and Waldron, B. (2007). Upland complex of the central Mississippi River valley: its origin, denudation, and possible role in reactivation of the New Madrid Seismic Zone. In *Continental Intraplate Earthquakes: Science, Hazard, and Policy Issues*, ed. S. Stein, and S. Mazzotti. Geological Society of America Special Paper 425, 177.

Working Group on California Earthquake Probabilities (WGCEP) (2013). *Proposed Time-Independent Uniform California Earthquake Rupture-Forecast, Version 3.1 (UCERF3.1)*. Report delivered to California Earthquake Authority.

Wu, P., and Johnston, P. (2000). Can deglaciation trigger earthquakes in North America? *Geophysical Research Letters*, 27, 1323–1326.